International Journal of Pharmaceutics 371 (2009) 99–105

Contents lists available at ScienceDirect

International Journal of Pharmaceutics

journal homepage: www.elsevier.com/locate/ijpharm

Influence of realistic airflow rate on aerosol generation by nebulizers

Laurent Vecellio[a,*], Paul Kippax[b,1], Stephane Rouquette[c,2], Patrice Diot[d,e,f,3]

[a] Aerodrug, Faculté de Medecine, Tours, F-37000 France
[b] Malvern Instruments Limited, Enigma Business Park, Grovewood Road, Malvern, Worcestershire, WR5 3RL, UK
[c] Malvern Instrument SA, Parc Club de l'Université, 30 rue Jean Rostand, 91893 Orsay Cedex, France
[d] Inserm U 618, Tours, F-37000 France
[e] IFR 135, Tours, F-37000 France
[f] Université François Rabelais de Tours, F-37000 France

ARTICLE INFO

Article history:
Received 1 February 2008
Received in revised form
22 September 2008
Accepted 18 December 2008
Available online 27 December 2008

Keywords:
Laser
Size
Concentration
Nebulizer
Aerosol

ABSTRACT

Mathematical models are available which predict aerosol deposition in the respiratory system assuming that the aerosol concentration and size are constant during inhalation. In this study, we constructed a sinusoidal breathing model to calculate the aerosol concentration produced by a nebulizer as a function of inhalation time. The laser diffraction technique (Spraytec™, Malvern Instruments Ltd., Malvern, UK) was used to validate this model as it allows the aerosol concentration and particle size to be measured in real time. Each nebulizer was attached to a special glass measurement cell and a sine-wave pump. Two standard jet nebulizers (Mistyneb® and Microneb®), two breath-enhanced jet nebulizers (Pari® LC+ and Atomisor® NL9 M) and three mesh nebulizers (Eflow®, Aeroneb® Go and Aeroneb® Pro with Idehaler®) were characterized. Results obtained were consistent in terms of curve profile between the proposed model and the laser diffraction measurements. The standard jet and mesh nebulizers produced significant variations in aerosol concentration during inhalation, whereas the breath-enhanced jet nebulizers produced a constant aerosol concentration. All of the nebulizers produced a relatively constant particle size distribution. Our findings confirm that the concentration observed during inhalation is often not constant over time. The laser diffraction method allows the concentration and size of particles for each unit volume of air inhaled to be measured and could therefore be used to predict the aerosol deposition pattern more precisely.

1. Introduction

Algorithms for modeling aerosol deposition in the respiratory tract have been developed in the past, primarily with the objective of predicting the exposure risks associated with working in hazardous environments (e.g. when working with radioactive materials) (ICRP, 1994). For several years, these models have also been used to predict the behavior of medical aerosols (Fleming et al., 2006), making it possible to understand the effect of parameters such as particle size, patient anatomy, ventilation, exposure time and concentration on drug deposition within the respiratory system (ICRP, 1994; Asgharian et al., 2001). However, each of the available models assumes that the aerosol concentration and size are constant during inhalation (Freijer et al., 1999; Jarvis et al., 1996). Although this is a reasonable assumption for airborne contaminants, it is not true for many medical aerosols. For example, Coates et al. (2001) described a mathematical model for a standard jet nebulizer showing different levels of dilution of the aerosol during inhalation. Other models have been developed to predict the operation of breath-enhanced jet nebulizers in terms of output (Katz et al., 2001; Ho et al., 2001; Leung et al., 2007; Chatburn and McPeck, 2007) and particle size (Katz et al., 2001; Ho et al., 2001; Leung et al., 2007) as a function of airflow rate, but these models can be difficult to apply to other jet nebulizer designs (Leung et al., 2004).

Aerosol concentration and droplet size can be measured experimentally during inhalation as an alternative to modeling nebulizer operation. The aerosol concentration can be derived by a mass balance method (Coates et al., 1998), calculated as the ratio of the nebulizer output to the inhalation airflow rate. This method has the advantage of allowing the concentration of the active pharma-

* Corresponding author at: Aerodrug, Bat M, Faculté de Médecine, 10 Bld Tonnellé, 37032 TOURS cedex, France. Tel.: +33 247366061; fax: +33 247366196.
E-mail addresses: vecellio@med.univ-tours.fr (L. Vecellio), Paul.Kippax@malvern.com (P. Kippax), stephane.rouquette@malvern.com (S. Rouquette), diot@med.univ-tours.fr (P. Diot).
[1] Malvern Instruments Ltd., Enigma Business Park, Grovewood Road, Malvern, WR5 3RL, UK. Tel.: +44 1684 892456; fax: +44 1684 892789.
[2] Malvern Instruments SA, Parc Club de l'Université, 30 Rue Jean Rostand, 91893 Orsay Cedex, France. Tel.: +33 1 6935 1800; fax: +33 1 6019 1326.
[3] CHRU Bretonneau, 37044 TOURS Cedex, France. Tel: +33 247478032; fax: +33 2247479173.

0378-5173/$ – see front matter © 2009 Elsevier B.V. All rights reserved.
doi:10.1016/j.ijpharm.2008.12.027

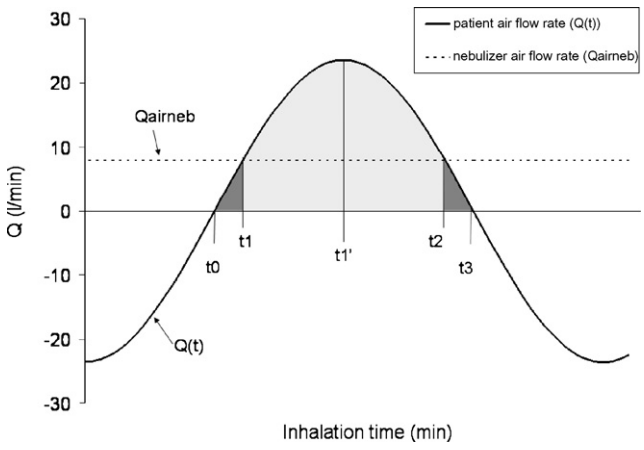

Fig. 1. Diagram of a patient inhaling ($Q(t)$) an aerosol produced by a jet nebulizer operating continuously with an airflow (Q_{airneb}).

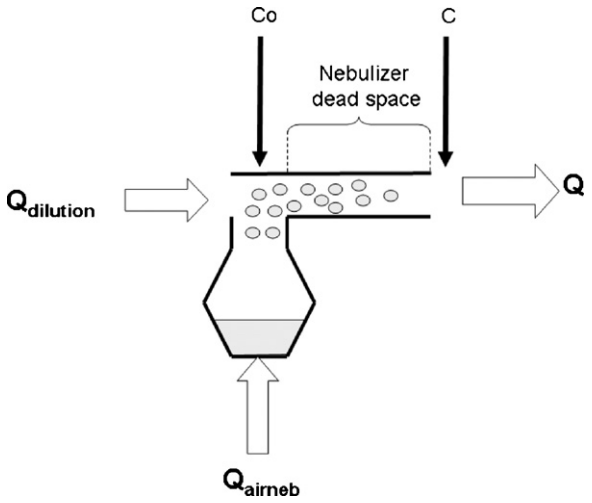

Fig. 2. Nebulizer operation with special "T" piece. $Q(t)$, airflow rate inhaled by the patient; Q_{airneb}, airflow rate source for the nebulizer; Q dilution, airflow rate of ambient air diluting the aerosol when $Q(t) > Q_{airneb}$.

ceutical ingredient (API) in the aerosol to be measured. However, it does not allow the concentration at different time points during inhalation to be obtained nor does it take into account the breathing profile of the patient (i.e. inhalation and exhalation phases), which can be important for nebulizers where the aerosol is stored within the device during exhalation. On the other hand, photometry techniques allow the concentration to be measured at different time points of the inhalation (Gebhart et al., 1988). Such methods have been used with monodisperse aerosols to determine the pulmonary aerosol deposition patterns in patients (Gebhart et al., 1988; Darquenne et al., 1997; Kim and Hu, 2006; Kim et al., 1996; Clark et al., 2007). However, the photometry method cannot be used to calculate real-time particle size distributions.

One technique that does provide the potential for measuring both aerosol concentration and particle size is laser diffraction. In the past, Ho et al. (2001) used this method to measure the airflow rate dependence of the particle size produced by nebulizers. The method used at that time did not allow the real-time measurement of the particle size during inhalation nor did it mimic exactly the breathing profile of a typical patient.

The aim of this study was to build on the work of Ho et al. (2001) by using the Spraytec™ laser diffraction system (Malvern Instruments Ltd., Malvern, UK) as this system can simultaneously measure the aerosol concentration and size produced by any nebulizer during a typical inhalation manoeuvre. The first step was to model the aerosol concentration inhaled by a patient with a standard jet nebulizer and to compare it to our experimental results in order to validate the experimental measurement method. The second step was to measure the change of aerosol concentration and particle size produced by different kinds of nebulizer during the inhalation phase and to analyze its potential influence on the prediction of aerosol deposition.

2. Materials and methods

2.1. Mathematical modeling

2.1.1. Theory

2.1.1.1. Theory without nebulizer dead space. A mathematical model was constructed to calculate the aerosol concentration delivered by a nebulizer as a function of time during inhalation.

The airflow rate inhaled by the patient (Q) was modeled by a sinusoidal function (Fig. 1) as a function of (t):

$$Q = Qo\sin(wt) \quad (1)$$

$$\text{With } Qo = \frac{(V_T w)}{2}; \quad w = \frac{(\pi f)}{(T_i/T_{tot})};$$

where V_T is the tidal volume; f, the respiratory rate per minute; T_i, the inhalation time during one breath and T_{tot}, the time for one breath.

The second part of our mathematical model was based on the work of Coates et al. (2001) and was developed to predict the concentration changes occurring during the delivery of an aerosol from a standard jet nebulizer via a T piece (Fig. 2) specially designed to limit aerosol storage at the beginning of the inhalation phase in order to simplify the model. The concentration (C) was defined as the ratio between the volume of particles (V_{part}) and the air volume (V_{air}) containing the particles, i.e., $C = V_{part}/V_{air}$. Assuming that the nebulizer produces a constant output (Q_{neb}) during inhalation (11), two modes of operation can be defined:

- When the patient-induced flow rate (Q) is lower than the gas flow rate used to drive the nebulizer (Q_{airneb}), there is no aerosol dilution ($t0 < t < t1$; $t2 < t < t3$). The aerosol concentration is constant and can be expressed as follows: $Co = Q_{neb}/Q_{airneb}$; $Q < Q_{airneb}$.
- When the patient-induced flow rate (Q) is higher than the gas flow rate used to drive the nebulizer (Q_{airneb}), the aerosol is diluted by air drawn in from the environment ($Q_{dilution} = Q - Q_{airneb}$) ($t1 < t < t2$). The aerosol concentration is therefore not constant and can be expressed as follows: $Co = Q_{neb}/Q$; $Q > Q_{airneb}$

2.1.1.2. Theory with nebulizer dead space. This theory presents an aerosol concentration model produced by a standard jet nebulizer with a dead space (Fig. 2). The reasoning of the calculation is based on the moving volume of aerosol. We hypothesize that there is no loss of aerosol in the dead space.

The dead space (V_{dead}) for a nebulizer can be defined as the volume between the extremity of the nebulizer delivering the aerosol to the patient (e.g. extremity of mouth piece) and where the aerosol is generated (e.g. 10 ml).

When the patient begins to inhale, the first part of air volume is clear of aerosol due to the nebulizer's dead space. So, when V is smaller than V_{dead}: $C = 0$ ($C = 0$; $V < V_{dead}$).

In the second part of the inhaled air, the aerosol is produced with a constant concentration ($C = Q_{neb}/Q_{airneb}$) until a time $t1$.

Based on Fig. 1 and on the theory section, the boundary condition is $Q(t) = Q_{neb}$.

Resolving this equation, we obtain two solutions: $t1$ and $t2$

$$t1 = \frac{1}{w}\sin^{-1}\left(\frac{Q_{airneb}}{Q_o}\right)$$

$$t2 = \frac{1}{w}\left(\pi - \sin^{-1}\left(\frac{Q_{airneb}}{Q_o}\right)\right)$$

A fraction of this aerosol has already been produced in the dead space and is inhaled by the patient until the inhalation of the volume $V(t1)+V_{dead}$ ($V<V(t1)+V_{dead}$).

In the third part of the inhaled air, the aerosol is diluted by the ambient air until the time $t2$ (Fig. 1). A fraction of this aerosol has already been produced in the dead space and is inhaled by the patient until the inhalation of the volume $V(t2)+V_{dead}$ ($V<V(t2)+V_{dead}$). The concentration inhaled by the patient is:

$$C = \frac{Q_{neb}}{Q}$$

Q is not the airflow rate at the "t" time (due to the dead space) but the airflow rate at a previous time. To resolve this problem, Q is expressed as a function of V.

By resolving this equation system,

$$\begin{cases} Q = Q_o \sin(wt) \\ V = \dfrac{V_T}{2}(1-\cos(wt)) \end{cases}$$

We obtain:

$$Q = Q_o \sin\left(\cos^{-1}\left(1-\frac{2V}{V_T}\right)\right)$$

Therefore, the concentration inhaled at the V volume is the concentration produced when the flow rate was produced in the $V-V_{dead}$ volume before. Thus, we obtain:

$$C = \frac{Q_{neb}}{[Q_o \sin(\cos^{-1}(1-2(V-V_{dead})/V_T))]}$$

In the last part of the inhaled air ($V>V(t2)+V_{dead}$), the aerosol is produced with a constant concentration: $C=Q_{neb}/Q_{airneb}$.

To summarize:

$$\begin{cases} C = 0;\ V \le V_{dead} \\ C = \dfrac{Q_{neb}}{Q_{airneb}};\ V_{dead} \le V \le V(t1)+V_{dead} \\ C = \dfrac{Q_{neb}}{Q_o \sin(\cos^{-1}(1-\frac{2(V-V_{dead})}{V_T}))};\ V(t1)+V_{dead} \le V \le V(t2)+V_{dead} \\ C = \dfrac{Q_{neb}}{Q_{airneb}};\ V(t2)+V_{dead} \le V \le Vt \end{cases}$$

2.1.2. Simulation

The theoretical concentration profile was calculated for a patient breathing at an inhalation time of 1.29 ± 0.03 s with a 500 ± 15 ml tidal volume. A standard jet nebulizer fitted with a T piece was used to simulate the concentration profile. The T piece was specially designed to avoid aerosol storage at the end of the exhalation. The nebulizer was operated at a compressed airflow rate of 8.5 ± 0.75 l min^{-1} (Q_{airneb}) and calculations were done for 0 and 10 ml nebulizer dead space. The concentration inhaled by the patient was expressed in terms of inhalation time and the inhaled volume ($V(t) = \int_0^t Q(t)dt$, so $V(t)=V_T(1-\cos(wt))/2$, adapted from Coates et al. (2006)). Concentrations were normalized to obtain concentration distribution in term of time or inhaled volume.

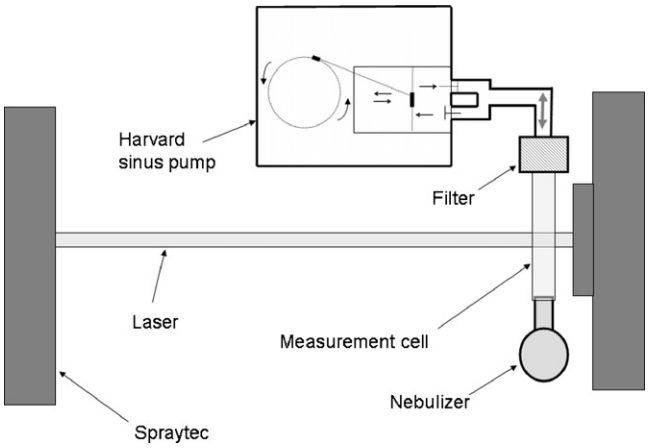

Fig. 3. Experimental set-up to measure aerosol concentration and size in real time.

2.2. Experimental measurement method

2.2.1. Experimental set-up

The nebulizer was attached to a special glass measurement cell as previously described (Vecellio None et al., 2001) and a modified sine-wave pump (Harvard, USA) (Fig. 3) set to deliver 20 breaths per minute with a tidal volume of 500 ml and a 40:60 inspiration to expiration ratio. A filter was connected close to the end of the measurement cell to minimize the risk of measuring the "exhaled" aerosol. The Spraytec™ laser diffraction system (Malvern Instruments Ltd.) was used to measure the particle size distribution and the concentration of the aerosol introduced into the measurement cell. The measurement cell was placed close to the Spraytec's collection lens and in a horizontal position to allow the laser to pass through the cell. In addition, in order to limit interference between the light transmitted by the laser source and the light refracted from the sides of the glass cell, the cell was positioned so that the two principal refraction patterns were not coincident with the laser source. The background light scattering observed from the cell in the absence of the aerosol was recorded before each measurement.

2.2.2. Nebulizers

A standard Microneb® jet nebulizer fitted with the special T piece (10 ml dead space) described above was tested using a compressed air supply of 8.5 l min^{-1}. Concentration results were normalized taking into account the 10 ml dead space to calculate the inhalation time (1.17 vs. 1.29 s). Results were then compared to the predictions of our mathematical model. The output of several commercial nebulizer devices was then characterized using the laser diffraction system. Two jet nebulizers were characterized using classical T pieces and a compressed air supply of 8 l min^{-1}: a Microneb® nebulizer (Europe Medical, Bourg-en-Bresse, France) and a Mistyneb® nebulizer (Allegiance, France). Two breath-enhanced nebulizers were studied: a Pari® LC + nebulizer (Pari, Germany) fitted with a Turboboy compressor (Pari, Germany), and an Atomisor® NL9 M nebulizer (La Diffusion Technique Française, France) fitted with an Abox + compressor (La Diffusion Technique Française, France). Finally, three mesh nebulizers were characterized: an eFlow® Rapid nebulizer (Pari, Germany), an Aeroneb®-Go nebulizer (Nektar therapeutics-Aerogen, USA) and a new nebulizer using the Idehaler® vertical holding chamber (La Diffusion Technique Française, France) with an Aeroneb® Pro nebulizer (Nektar therapeutics-Aerogen, USA). Each nebulizer was tested six times using 3 ml of saline isotonic solution.

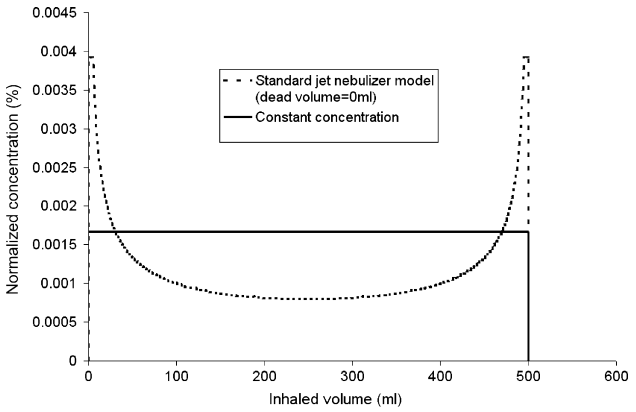

Fig. 4. Comparison in terms of normalized concentration during the inhalation volume (sinus airflow rate) between the simulation obtained with a standard jet nebulizer (dead space = 0 ml) and the hypothesis of a constant concentration.

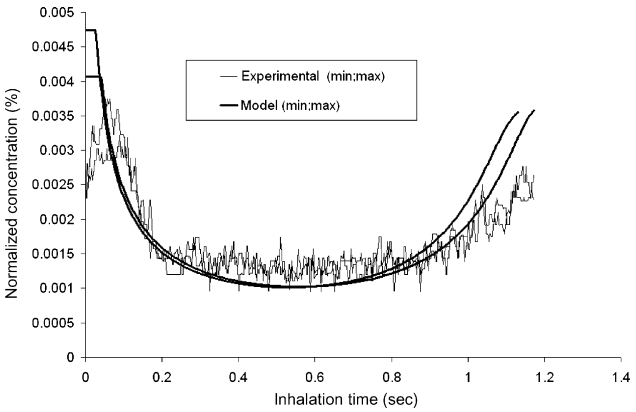

Fig. 5. Comparison in terms of normalized concentration during the inhalation time (sinus airflow rate) between the simulation obtained with the Microneb jet nebulizer (dead space = 10 ml) and the experimental data.

2.2.3. Measurement Method

The aerosol concentration and particle size were measured every 2 ms (500 Hz) using the Spraytec laser diffraction system (Malvern Instruments Ltd). The scattering data obtained by the system was analyzed using the Mie scattering model, with the refractive index of the continuous phase set to 1 (air), the refractive index of the particulate phase set to 1.33 (water) and the imaginary refractive index of the particulate phase set to 0 (transparent particles). In addition, Beer–Lambert's law was used to calculate the spray concentration based on the changes in laser light transmission observed during nebulization and the geometry of the measurement cell (path length = 8 cm).

Six consecutive measurements were carried out and the average concentration and MMAD profiles associated with each inhalation manoeuvre were calculated. In addition, the product between the concentration (C) and the fine particle fraction (Leung et al., 2007) (FPF, volume percentage of particles less than 5 μm) was calculated in order to determine the fine particle concentration delivered at each time point. This is considered to be an accurate measurement of the volume of particles produced by the nebulizer entering the airways without depositing in the mouth or throat.

3. Results

3.1. Simulation

Fig. 4 shows the concentration data generated by the simulation model for the standard jet nebulizer as a function of inhalation volume. It suggests that the aerosol concentration is not constant, with a variation factor of 4 in concentration between the beginning and the middle of the inhalation cycle. For the first part of the concentration profile ($t0$ and $t1$), the inhaled aerosol concentration is constant because there is no aerosol dilution ($Q < Q_{airneb}$). Within the second part of the profile ($t1$ and $t1'$), the concentration of the inhaled aerosol decreases because of the dilution of the aerosol and the increase in the inhaled flow rate ($Q > Q_{airneb}$, $Q < Q_{oi}$). During the third part of the profile ($t1'$ and $t2$), the concentration increases because the inhaled flow rate decreases ($Q > Q_{airneb}$ and $Q > Q_{oi}$). Finally for the standard jet nebulizer without dead volume, during the final part of the profile ($t2$ and $t3$), the aerosol concentration is constant because there is no further aerosol dilution ($Q < Q_{airneb}$).

Assuming that the aerosol flows perfectly into the airways without aerosol deposition within the anatomic dead space, it is possible to predict the concentration of aerosol delivered to each part of the airway. The profile obtained from the simulation with the standard jet nebulizer without dead volume suggests that a high aerosol concentration is delivered to the alveolar region (0–50 ml inhaled volume) and the upper airways (450–500 ml inhaled volume), whereas a lower concentration is delivered between these two regions (50–450 ml inhaled volume). This result is in contrast with the constant concentration hypothesis, which suggests an aerosol concentration distribution constant in each part of the airway (Fig. 4).

3.2. Validation of the experimental measurement method

To validate our experimental measurement set-up, we compared our simulation to the results obtained using laser diffraction. Fig. 5 shows the normalized concentration as a function of time obtained from the Microneb® device when using the same nebulization conditions and breathing profile as in the simulation. The profile changes observed in the measured concentration were found to be consistent with the proposed model. Therefore, the experimental measurement method, validated by our model, can be used to measure different concentration profiles. Moreover, as our measurement cell had previously been validated for measuring the particle size distribution produced by different nebulizer systems (Vecellio None et al., 2001), it was possible to determine the concentration of aerosol delivered at each particle size for different kinds of nebulizers.

3.3. Experimental results

Fig. 6 shows the concentration profile obtained using laser diffraction for the two standard jet nebulizers and the two breath-enhanced jet nebulizers described above.

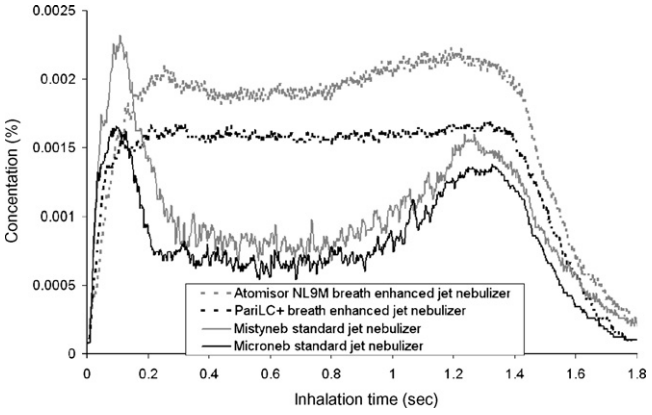

Fig. 6. Aerosol concentration results during the inhalation phase with different jet nebulizers and a sinus airflow rate (500 ml, 40/60, 20/min).

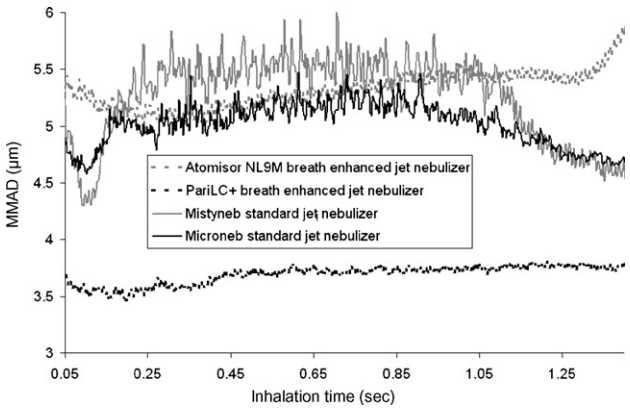

Fig. 7. MMAD results during the inhalation phase with different jet nebulizers and a sinus airflow rate (500 ml, 40/60, 20/min). MMAD between 0.05 and 1.4 s of inhalation time revealing the good obscuration to obtained a confident measurement.

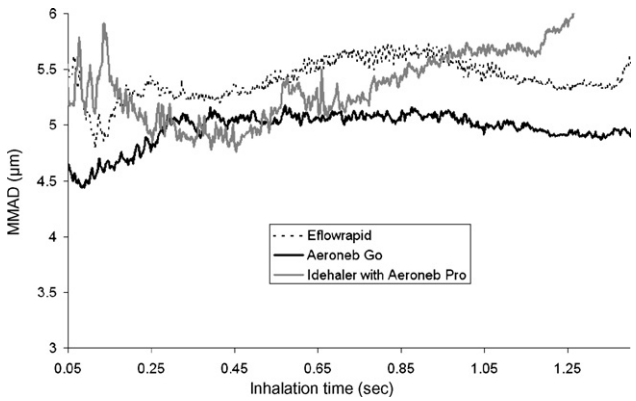

Fig. 9. MMAD results during the inhalation phase with different mesh nebulizers and a sinus airflow rate (500 ml, 40/60, 20/min). MMAD between 0.05 and 1.4 s of inhalation time revealing the good obscuration to obtained a confident measurement.

The two standard nebulizers produced a continuously varying aerosol concentration during patient inhalation (a variation factor of 3), whereas the two breath-enhanced jet nebulizers produced a relatively constant aerosol concentration during the mid-point of the inhalation profile. MMAD produced by these devices was also stable during the mid-point of the inhalation phase (Fig. 7). This is in contrast to the standard jet nebulizers, which are characterized by a small increase in MMAD observed as the aerosol is diluted by ambient air drawn into the device (from 4.3 to 5.9 μm for Mistyneb® nebulizer and from 4.6 to 5.5 μm for Microneb® nebulizer). On average, during the whole inhalation phase, the Microneb® produced an aerosol with a MMAD of 5.0 ± 0.2 μm, the Mistyneb® a MMAD of 5.2 ± 0.4 μm, the Pari® LC + a MMAD of 3.7 ± 0.1 μm, and the Atomisor® NL9 M a MMAD of 5.3 ± 0.1 μm.

Fig. 8 shows the results in terms of concentration profile for the mesh nebulizers. There was a variation in the concentration of the aerosol during patient inhalation with all mesh nebulizers. The Eflow® rapid produced the highest concentration at the beginning of the inhalation, followed by a sharp tail-off in concentration as the flow rate increased. Towards the end of the profile, a small increase of the aerosol concentration was observed. The Aeroneb® Go nebulizer produced a similar profile to the Eflow® rapid, but the profile shifted to much lower aerosol concentrations variation. Finally, the Idehaler® used with the Aeroneb® Pro was characterized by a steady increase in aerosol concentration during the first part of the inhalation profile, followed by a gradual decrease in concentration during the second part of the inhalation profile.

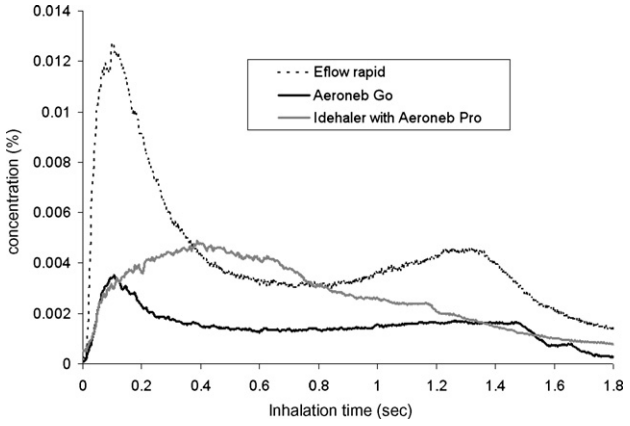

Fig. 8. Aerosol concentration results during the inhalation phase with different mesh nebulizers and a sinus airflow rate (500 ml, 40/60, 20/min).

A relatively constant aerosol MMAD (Fig. 9) was observed with the mesh nebulizers at the mid-point of the inhalation profile. The Aeroneb® Go and Eflow® rapid nebulizers displayed similar characteristics to the standard jet nebulizers, with a small increase in the MMAD observed as the flow rate increased towards the mid-point of the inhalation profile (from 4.5 to 5.1 μm for Aeroneb® Go and from 4.8 to 5.7 μm for Eflow® rapid). This is the time period during which aerosol dilution occurs. In contrast, the Aeroneb® Pro fitted with the Idehaler® spacer showed an increase in MMAD during the second part of the inhalation phase (from 4.8 to 6 μm) – this was also associated with dilution of the aerosol. On average, throughout the whole inhalation cycle, the Eflow® rapid nebulizer produced an aerosol with a MMAD of 5.4 ± 0.2 μm, the Aeroneb® Go a MMAD of 5.0 ± 0.2 μm, and the Aeroneb® Pro fitted with the Idehaler® spacer a MMAD of 5.3 ± 0.3 μm.

Finally, FPF concentration profiles (data not shown) and concentration profiles for jet and mesh nebulizers followed a similar trend.

4. Discussion

By using a mathematical model, we demonstrate that the concentration produced by a standard jet nebulizer is not constant during realistic inhalation (Fig. 4). As a consequence, the volume of particles contained within each unit volume of air inhaled by the patient changes during the inhalation phase and is related to the airflow rate induced by the patient. These mathematical data were confirmed by the experiment using laser diffraction, a technique that allows the aerosol concentration to be measured at 2 ms time intervals during the inhalation cycle. When using a sinusoidal breathing profile to model patient inhalation (500 ml, 20/min, 40/60), the normalized concentration changed by a factor of 4 during the inhalation phase with less aerosol being delivered at the mid-point than at the beginning and end of inhalation. Moreover, the normalized concentration observed towards the end of the inhalation phase did not fit the proposed model exactly. These differences can be explained by the operation mode of the pump, as it is difficult to produce a perfect sine-wave profile in terms of airflow rate and to control the inhalation parameters exactly. Our study produced similar results for different standard jet nebulizers, whereas breath-enhanced jet nebulizers produced a constant aerosol concentration during the inhalation phase. Our results are consistent with those of Katz et al. (2001) who identified a quadatric relationship between the airflow rate and aerosol output produced by jet nebulizers. By contrast, the Pari® LC + breath-enhanced jet nebulizer produced relatively constant aerosol concentration (Fig. 6),

indicating an almost linear relationship between airflow rate and aerosol output (Ho et al., 2001). Our experimental results also show that the two breath-enhanced jet nebulizers (Pari® LC + and Atomisor® NL9 M) produced a more constant aerosol concentration during inhalation than the two standard jet nebulizers (Microneb® and Mistyneb®). This difference is related to the different operating modes of each device. Breath-enhanced jet nebulizers use the patient's inhalation airflow rate to increase the rate of aerosolization during the inhalation phase, hence the aerosol concentration tends to be independent of the airflow rate generated by the patient during inhalation.

The three mesh nebulizers tested differed in terms of concentration profile and produced more aerosol during the first part of inhalation. The concentration profile obtained for the Eflow® rapid can be explained by the fact that it has a 30 ml aerosol holding chamber (Vecellio, 2006). During exhalation, the aerosol produced by the device is stored in this chamber and is released once the inhalation phase begins. This causes a high initial aerosol concentration (Fig. 8). The increase in the aerosol concentration at the end of the inhalation cycle can be explained by a similar mechanism, as seen for the standard jet nebulizers. When the Eflow® holding chamber is clear of aerosol, the nebulizer operates like a standard jet nebulizer, with the air drawn through the device causing dilution. Once the airflow rate starts to decrease towards the end of the inhalation profile, the aerosol concentration increases.

The Aeroneb® Go mesh nebulizer behaved in a similar way to the Eflow® rapid nebulizer delivering a high concentration of aerosol at the beginning of the inhalation cycle. However, the concentration observed was not as high (Fig. 8). This can be explained by the difference in aerosol flow produced by the mesh and the operating mode of the nebulizers. The Aeroneb® Go mesh nebulizer can be compared to a standard jet nebulizer in terms of its mode of operation, i.e., it provides a constant source of aerosol particles, which are diluted by the airflow induced by the patient. There is no chamber to store the aerosol produced during the exhalation phase, thus the concentration increase observed is due to the storage of aerosol in the dead space within the device at the end of the inhalation rather than within a specific holding chamber. Following the initial part of the inhalation cycle, the concentration rapidly decreases and then gradually increases towards the end of inhalation (Fig. 8). Aeroneb® Pro operating with the Idehaler® chamber operates like the Eflow® rapid but with a vertical chamber. This new device also showed a high concentration during the first part of inhalation but a continuous decrease in aerosol at the end of inhalation (Fig. 8).

The MMAD produced by the mesh nebulizers increased when concentration decreased (Fig. 9). This increase could have resulted from an artefact induced by the measurement method, since the deposition of large particles on the glass of the measurement cell could have an influence on the measurement for low aerosol concentration. The change in MMAD could also be accounted for by the way the nebulizer operates; for example, the large particles produced at the end of the inhalation phase with the Aeroneb® Pro operating with the Idehaler® chamber could be due to sedimentation and the effect of transport. During the exhalation phase, aerosol is produced in the Idehaler®, with the largest particles at the bottom. During the next inhalation, the largest particles are transported out of the chamber after the smallest particles.

Results also suggest that aerosol droplet coalescence does not occur within the holding chambers used to concentrate the aerosol during exhalation. However, the variability of the MMAD produced during inhalation by the jet and mesh nebulizers is not as pronounced as the variability observed in the aerosol concentration. For example, with the Microneb® nebulizer, the concentration changed by 238% during the inhalation phase, whereas the MMAD changed by a maximum of 28%. Moreover, if we consider the product between the concentration and the FPF, profiles (data not shown) obtained are consistent with the concentration profiles, suggesting that the concentration is a more important factor in differentiating the performance of the nebulizers tested here. Assuming that the product between the FPF and the concentration correlates with the volume of particles, which may penetrate the airways without deposition in the mouth or throat, concentration profiles show the distribution of the aerosol penetration in the airways at the end of the inhalation phase.

These results provide new information about the process of aerosol kinetics in the airways and demonstrate the importance of measuring the aerosol in real time. It also allows the efficacy of delivery to be compared for nebulizers producing a continuous stream of aerosol particles and those producing higher aerosol concentrations during the first part of the inhalation profile as a means of increasing intrathoracic deposition (Bennett et al., 1998). The aerosol concentration and size, which penetrates into the different parts of the airways, could be calculated by an increment method (Coates et al., 2001). Thus, a comparison of the performance of different nebulizers and prediction of aerosol deposition could be realized with more precision. This calculation cannot yet be realized using the set-up described here, because we need to synchronize the laser diffraction measurement (concentration and size) with a pneumotachograph (airflow rate) in order to precisely measure the concentration and size of particles in each unit of inhaled volume. Moreover, this time synchronization would avoid any measurement artifacts caused by the nebulizer dead space and the incomplete clearance of cell measurement during exhalation.

In conclusion, the concentration produced by nebulizers during inhalation is often not constant. The measurement method presented here has the advantage of allowing simultaneous measurement of the aerosol concentration and particle size distribution for each unit of inhalation time during the inhalation phase (which is not constant in terms of flow rate). It also allows aerosolization to be monitored in a situation where the applied flow rate mimics the processes of exhalation and inhalation, which can be important for nebulizers where aerosol is retained within the device during exhalation, either with a dead space or a specific storage volume. However, our method does not allow the active drug concentration contained within the droplets produced by the nebulizer to be measured. Associated with an assaying method (e.g. a filtering method), the method could provide more precise information about aerosol parameters in order to predict its deposition.

Disclosure statement

Laurent Vecellio is an inventor of the Idehaler®.Aerodrug is a department of La Diffusion Technique Française, France.

Paul Kippax and Stephane Rouquette are in full-time employment with Malvern.

No conflicts of interest exists for Patrice Diot.

References

Asgharian, B., Hofmann, W., Bergmann, R., 2001. Particle deposition in a multiple-path model of the human lung. Aerosol. Sci. Technol. 34, 332–339.

Bennett, W.D., Scheuch, G., Zeman, K.L., Brown, J.S., Kim, C., Heyder, J., Stahlhofen, W., 1998. Bronchial airway deposition and retention of particles in inhaled boluses: effect of anatomic dead space. J. Appl. Physiol. 85, 685–694.

Chatburn, R.L., McPeck, M., 2007. A new system for understanding nebulizer performance. Respir. Care 52, 1037–1050.

Clark, A.R., Chambers, C.B., Muir, D., Newhouse, M.T., Paboojian, S., Schuler, C., 2007. The effect of biphasic inhalation profiles on the deposition and clearance of coarse bolus aerosols. J. Aerosol. Med. 20, 75–82.

Coates, A.L., Allen, P.D., MacNeish, C.F., Ho, S.L., Lands, L.C., 2001. Effect of size and disease on estimated deposition of drugs administered using jet nebulization in children with cystic fibrosis. Chest 119, 1123–1130.

Coates, A.L., MacNeish, C.F., Lands, L.C., Meisner, D., Kelemen, S., Vadas, E.B., 1998. A comparison of the availability of tobramycin for inhalation from vented vs. unvented nebulizers. Chest 113, 951–956.

Coates, A.L., Tipples, G., Leung, K., Gray, M., Louca, E., 2006. How many infective viral particles are necessary for successful mass measles immunization by aerosol? Vaccine 6, 1578–1585.
Darquenne, C., Brand, P., Heyder, J., Paiva, M., 1997. Aerosol dispersion in human lung: comparison between numerical simulations and experiments for bolus tests. J. Appl. Physiol. 83, 966–974.
Fleming, J.S., Epps, B.P., Conway, J.H., Martonen, T.B., 2006. Comparison of SPECT aerosol deposition data with a human respiratory tract model. J. Aerosol Med. 19, 268–278.
Freijer, J.I., Cassee, F.R., Subramaniam, R., Asghararian, B., Anjilvel, S., Miller, F.J., Bree van, L., Rombout, P.J.A. 1999. Multiple Path Particle Deposition Model (MPPDep Version 1.11). A model for human and rat airway particle deposition. RIVM Report 650010019. National Institute for Public Health and the Environement (RIVM). Chemical Industry Institute of Toxicology (CIIT). Bithoven, The Netherlands.
Gebhart, J., Heicwer, G., Heyder, J., Roth, C., Stahlhofen, W., 1988. The use of light scattering photometry in aerosol medicine. J. Aerosol Med. 2, 89–112.
Ho, S.L., Kwong, W.T., O'Drowsky, L., Coates, A.L., 2001. Evaluation of four breath-enhanced nebulizers for home use. J. Aerosol Med. 14, 467–475.
ICRP (International Commission for Radiological Protection), 1994. ICRP Publication 66. Human Respiratory Tract Model for Radiological Protection. Pergamon Press, Oxford, UK.
Jarvis, N.S., Birchall, A., James, A.C., Bailey, M.R., Dorrian, M.-F., 1996. LUDEP 2.0 Personal Computer Program for Calculating Internal Doses Using the ICRP Publication 66 Respiratory tract Model. National Radiological Protection Board, Chilton, UK.
Katz, S.L., Ho, S.L., Coates, A.L., 2001. Nebulizer choice for inhaled colistin treatment in cystic fibrosis. Chest 119, 250–255.
Leung, K., Louca, E., Coates, A.L., 2004. Comparison of breath-enhanced to breath-actuated nebulizers for rate, consistency, and efficiency. Chest 126, 1619–1627.
Leung, K., Louca, E., Munson, K., Dutzar, B., Anklesaria, P., Coates, A.L., 2007. Calculating expected lung deposition of aerosolized administration of AAV vector in human clinical studies. J. Gene Med. 9, 10–21.
Kim, C.S., Hu, S.C., DeWitt, P., Gerrity, T.R., 1996. Assessment of regional deposition of inhaled particles in human lungs by serial bolus delivery method. J. Appl. Physiol. 81, 2203–2213.
Kim, C.S., Hu, S.C., 2006. Total respiratory tract deposition of fine micrometer-sized particles in healthy adults: empirical equations for sex and breathing pattern. J. Appl. Physiol. 101, 401–412.
Vecellio, L., 2006. The mesh nebulizer, a recent technical innovation for aerosol delivery. Breathe 2, 252–260.
Vecellio None, L., Grimbert, D., Becquemin, M.H., Boissinot, E., Le Pape, A., Lemarie, E., Diot, P., 2001. Validation of laser diffraction method as a substitute for cascade impaction in the European Project for a Nebulizer Standard. J. Aerosol Med. 14, 107–114.